General Disclaimer

One or more of the Following Statements may affect this Document

- This document has been reproduced from the best copy furnished by the organizational source. It is being released in the interest of making available as much information as possible.

- This document may contain data, which exceeds the sheet parameters. It was furnished in this condition by the organizational source and is the best copy available.

- This document may contain tone-on-tone or color graphs, charts and/or pictures, which have been reproduced in black and white.

- This document is paginated as submitted by the original source.

- Portions of this document are not fully legible due to the historical nature of some of the material. However, it is the best reproduction available from the original submission.

Produced by the NASA Center for Aerospace Information (CASI)

X-612-69-198

PREPRINT

NASA TM X-63562

OGO-4 SATELLITE MEASUREMENTS OF LOW ENERGY—HIGH LATITUDE ELECTRON PRECIPITATION

R. A. HOFFMAN

MAY 1969

GSFC

GODDARD SPACE FLIGHT CENTER
GREENBELT, MARYLAND

FACILITY FORM 602

N69-28245 (ACCESSION NUMBER) (THRU)
27 (PAGES) 1 (CODE)
NASA-TMX-63562 (NASA CR OR TMX OR AD NUMBER) 29 (CATEGORY)

OGO-4 SATELLITE MEASUREMENTS

OF LOW ENERGY - HIGH LATITUDE ELECTRON PRECIPITATION

By

R. A. Hoffman

NASA-Goddard Space Flight Center
Greenbelt, Maryland 20771

Paper presented at the NATO Advanced Study Institute, "Production and Maintenance of the Polar Ionosphere", Tretten, Norway, April 9-18, 1969.

ABSTRACT

Data from the Auroral Particles Experiment aboard OGO-4 have indicated four regions of low energy electron precipitation at high latitudes. These have been designated by the terms band region, burst region, polar cavity, and the pre-midnight region. The band region is characterized by a relatively structureless, moderately hard precipitation pattern which generally follows the auroral oval, except extends to lower latitudes at noon. It is especially prevalent in the dawn hemisphere. The burst region begins within the band region and extends polewards, reaching up to 85° at noon, and is characterized by usually a very soft spectrum and large structure in the precipitation pattern. The pitch angle distributions of 2.3 kev electrons within the bursts tend towards anisotropic, with the maximum flux directed along the magnetic field into the atmosphere. The polar cavity is an area of no detectable fluxes, while the pre-midnight region displays structured electron fluxes with widely varying spectra. This paper presents a preliminary summary of all the phenomena observed in the high latitude region and analyzed to date.

INTRODUCTION

Data from charged particle detectors capable of measuring fluxes of electrons whose energies are below a few kev indicate that there exists a region of precipitation of these low energy electrons poleward of the auroral oval (Sharp and Johnson, 1967; Burch, 1968; Hoffman and Evans, 1968; Hoffman, 1969). The influx of these electrons into the polar ionosphere can be an important energy source for various phenomena in this region (Maehlum, 1969; Burch, 1969).

The Auroral Particles Experiment aboard the Orbiting Geophysical Observatory (OGO) - 4 satellite has made measurements of these low energy electrons in the high latitude region for a period of 1½ years. This paper will present a preliminary summary of the phenomena observed in this region and analyzed to date.

EXPERIMENT

The satellite was launched on July 28, 1967, into a low altitude polar orbit having an apogee of 908 km, a perigee of 412 km, and an inclination of 86°. Orbital injection was into a dawn-dusk meridian plane. Precession of the orbit due to this inclination together with the motion of the earth around the sun cause a change in local time of the orbital plane of about 1½° per day.

The satellite was controlled in attitude such that one side of the spacecraft was always pointed towards the earth, while another axis was constrained to the earth, satellite, sun plane.

The Auroral Particles Experiment contains an array of eight detectors, each comprised of an electrostatic analyzer for species and

energy selection and a Bendix channel electron multiplier as the particle detector (Hoffman and Evans), 1967). Four of the detectors always point radially away from the earth (0°), while three others are positioned 30°, 60° and 90° to the earth-spacecraft radius vector (see Figure 1). Since the inclination of the earth's magnetic field is nearly 90° in the high latitude region the look directions sampled are very nearly the pitch angles of the particles detected. The eighth detector is a background detector.

The bandpass of each detector is +19%, -13% of the center energies indicated in Figure 1, while the geometric factor is about 6×10^{-5} cm^2-ster at the peak of the energy bandpass.

The sampling scheme of the detectors is also illustrated in Figure 1. The four energy detectors at 0° have their outputs accumulated simultaneously by four logarithmic digital accumulators for a time period of half the main telemetry frame before being read out, while during the second half of the main frame the four angle detectors, all measuring particles at 2.3 kev, have their pulse outputs accumulated simultaneously by the same accumulators before being read.

Since some of the data will be displayed in the figures as counting rates from the detectors, the conversion factors to fluxes are listed in Table 1. For additional details about the experiment, see Hoffman and Evans (1967).

DATA EXAMPLES

The data from the experiment at high latitudes indicate four distinct regions of low energy electron precipitation, each with its own characteristics as observed by the satellite detectors:

a. band region

b. burst region

c. polar cavity (Maehlum, 1969)

d. pre-midnight region

These terms are chosen as merely qualitative descriptions of the appearance of the data in the frame of reference of the moving satellite and are not meant to necessarily imply any true physical behavior on the part of the particles.

The first two regions of precipitation are shown in Figure 2, which contains data from a dusk to dawn pass which crossed magnetic local noon at a very high latitude. The relatively structureless, moderately hard precipitation at latitudes below 76° on the dawn side, especially noticeable in the 7.3 kev detector counting rate, is an example of what we term a band. Quite typically for the very low K_p period, of which this pass is an example (K_p = 0+), there is no detection of a dusk side band.

Well separated spatially on this pass and polewards of the band is the burst region, where usually the spectrum is very soft and the structure in the precipitation pattern in the frame of reference of the moving satellite is especially apparent at the lowest energy detected. This example of bursts is somewhat atypical in the sense that the 7.3 kev flux is larger than usual, but the entire pass is an excellent example of a complete polar crossing.

The precipitation in the pre-midnight region usually does not display this "two region" nature, as shown in Figure 3. Here, again for a low K_p pass (K_p=1-), the precipitation is very intense and structured even at 7.3 kev, and the spectrum is widely varying. Early and late in this

segment of data the 0.7 kev flux is three orders of magnitude larger than the 7.3 kev flux, while in some of the bursts this ratio is only a factor of 10.

The polar cavity appears as a region of no measureable precipitation by the experiment's detectors. For the first three weeks after launch the detector outputs were almost entirely free from noise, so an upper limit of a few counts/readout could be established over this region. During this period the upper limits on the flux in the energy range of the experiment are given as a few times the conversion factors listed in Table 1. (After three weeks in orbit a noise problem suddenly developed in the outputs of several of the detectors, so that very small fluxes could not be detected. This fairly steady noise output has since been diagnosed as a breakdown in the high voltage coupling capacitor. Unless otherwise indicated the noise has been subtracted from the counting rates plotted in the figures, and in no case was this noise level of any significance in the analyses discussed.)

BURST REGION

Because of the recent special interest in the trans-auroral zone region, the characteristics of the precipitating electrons in the burst region will be primarily discussed.

a. Structure.

Figure 4 shows in great detail the variations in the counting rates of two of the detectors while passing through the burst region. Since the abscissa marks occur every 10 seconds, the structure here appears to have time widths varying from less than one to a few seconds in the satellite frame of reference. The satellite is moving at about eight

kilometers/second. Of course, there is no way from the particle data alone to distinguish whether this precipitation is spatial or temporal in nature.

A very unusual seemingly monoenergetic burst is apparent in the 7.3 kev detector at 0619:20 U.T. Such higher energy bursts, though rare, always seem to occur while the lower energy detectors are measuring fairly high levels of radiation for some time or spatial interval around the higher energy burst. Assuming reasonable isotropy over the upper hemisphere, an assumption which will be shown later to be not necessarily tenable, this burst contained some 30 ergs/cm^2-sec of energy influx in the bandwidth of the 7.3 kev detector alone.

An even more detailed example of the distinctness which the bursts can attain is shown in Figure 5. This is the highest resolution data available from the spacecraft, and provides 55 sets of energy measurements and pitch angle distributions each second. The eight seconds of data in the figure begins with several bursts and ends in the region of a quiet band. Note the sharpness of each edge of the burst occurring at 0214:50.7 UT, especially the trailing edge, where the counting rate drops to a level only 30% of the peak rate in 18 milliseconds, or a distance traversed by the spacecraft of about 135 meters. The total width of the burst is only a quarter of a second, or an equivalent distance of 2000 meters.

b. Pitch Angle Distributions

An example of the pitch angle measurements during several bursts at the one energy of measurement appears in Figure 6. In the first burst,

marked "1", the 0° detector counting rate, sensitive to electrons with near 0° pitch angle, is considerably larger than the counting rates from the other three detectors, indicating an anisotropic pitch angle distribution with maximum flux directed along the magnetic field into the atmosphere. The very short burst, marked "2", was less than one main telemetry frame in length (about one-third second), and was similarly anisotropic. However, a few seconds later, the third burst appeared very isotropic. This is typical of the occurrence of anisotropic bursts: they exist in the minority and are interspersed with isotropic bursts.

The actual pitch angle distributions for the bursts marked "1" and "2" are shown in Figure 7.

c. Spectral Characteristics.

Energy spectra during bursts are impossible to classify. Usually the spectra are very soft so that the counting rate variations are most apparent at 0.7 kev, and the detector at that energy appears to be measuring the high energy tail of the precipitating electrons. The steepness of the spectra is indicated by the ratio of fluxes between 0.7 kev and 7.3 kev, which can reach as high as 10^4. At times, however, the spectrum of a burst hardens, and may even appear to be monoenergetic in terms of the energy resolution of the detector array, as illustrated by the 7.3 kev burst in Figure 4. In this case the 7.3 kev flux exceeded the 2.3 kev flux by a factor of six, and the 0.7 kev flux by 30%. Even within a burst the spectrum can vary widely. During the burst marked "1" in Figure 6, which lasted six data accumulation periods, the ratio between the 2.3 kev and 7.3 kev fluxes varied from 86:1 to 1:1.

d. Synoptic Parameters

Several parameters of the electron precipitation in the burst region are now studied in more detail in order to acquire a more comprehensive view of its properties.

i. Region and Probability of Occurrence

The first study is to define the region of occurrence of the electron bursts and determine the probability of occurrence within this region. For this purpose all data from July 30 through December 3, 1967, were analyzed. The data were divided into cells of invariant latitude and magnetic local time, $2\frac{1}{2}^{\circ}$ by one hour respectively, except for above 85°, where the cells were 5° by two hours. A cell was considered to be sampled if the path length of an orbit through the cell was at least one-half the dimension of the cell in the direction of travel. A cell was considered to have bursts if bursts existed over half of this path length. Thus there was no bias towards the existence of bursts. The criteria for bursts were rapid fluctuations in the counting rate from the 0.7 kev detector, with peak counting rates of at least 10^3 counts/sec (peak particle fluxes above about 10^8 electrons/cm^2-sec-ster-kev or peak energy fluxes above 10^{-1} ergs/cm^2-sec-ster-kev at 0.7 kev). The probability of occurrence of bursts in each cell was then calculated from the cumulative data. A cell was considered to be adequately sampled if four or more passes were made through it. The data were also separated into two levels of magnetic activity, divided at the value of K_p=2.

The map of the region and probability of occurrence for low magnetic activity is shown in Figure 8. Note the following features:

1. The bursts occur at all local times with no indication that the probability of occurrence is maximum at any local time.
2. At noon the region extends from 75° to 85°, whereas the northern boundary of the auroral oval lies at about 77° for low magnetic activity (Felstein et al., 1967).
3. Before 23 hours the average northern boundary, as distinguished by the jump from less than 20% occurrence to greater than 20%, occurs at about 80°, and there is a sudden displacement in the boundary 5° to the south after 23 hours.
4. In general the bursts begin within the auroral oval and extend well to the north of it.

Data from more magnetically disturbed periods is shown in Figure 9. The probabilities of occurrence in the heart of the burst region do not change appreciably, but the region of bursts shifts.

1. In the noon hemisphere the lower latitude boundary lies at least 5° to the equator side of the quiet time boundary.
2. The high latitude boundary in the noon hemisphere moves similarly by about $2\frac{1}{2}^{\circ}$.
3. There are indications that in the midnight regions there is an expansion in both directions of the latitude extent of the burst region.

i . Pitch Angle Distributions.

Examples of pitch angle distributions within individual bursts have shown the existence of both isotropic and field aligned

distributions at the single energy at which such measurements are made. In order to study the extent to which the bursts are observed to be field aligned, a scatter plot was made (Figure 10) of the total counts within the burst as measured by the 0° detector versus the total counts measured by the 60° detector.

Since the 0° detector is constrained to always point radially away from the earth, while the magnetic field vector is not inclined quite 90°, this detector usually measures particles with central pitch angles in the range from a few degrees to 10°, as is apparent from Figure 7. The detector itself accepts particles with pitch angles about $\pm 4^{\circ}$ around the central look angle.

Isotropic bursts have their data points lying near the line at 45° angle to the axes labeled "1X" in Figure 10. Note that all bursts lie either along this line or above it. Those lying above it show the field aligned character, with ratios between the fluxes at 0° and 60° of 2 and 5 indicated by the lines labeled "2X" and "5X" respectively. The maximum anisotropy shows a flux ratio of about eight.

The pitch angle distributions can be analyzed into two separate distributions (see Figure 7), an isotropic portion which always exists in all four angle detectors, and an anisotropic distribution which, when it appears, is manifest only in the 0° detector.

DISCUSSION

Some of the properties of the high latitude low energy electron precipitation have been presented in a preliminary summary form. One can

expect that these properties probably and in some cases certainly do depend upon various parameters of the magnetosphere, even without knowing the particle source mechanism. It has been shown that the high latitude boundary of the burst region is universal time controlled (Maehlum, 1968)(i.e., dependent upon the angle of the magnetic axis with the ecliptic plane), and is, therefore, also dependent upon the season of the year. While sequences of passes through the same local times may show similar precipitation patterns, there are also wide variations in the patterns and intensities between passes which are at least partially due to differences in magnetic activity. Indeed, it should be stressed that none of the statistical patterns of electron precipitation are necessarily applicable during polar substorms.

The source of these electrons is virtually unknown, although a consideration of the existence of the unique field aligned nature of some of the bursts has led to the suggestion that electric fields parallel to the magnetic field might be the acceleration mechanism (Hoffman and Evans, 1968). Because the field aligned portion of the precipitating fluxes always seems to be constrained to lie at angles less than about 30° to the field line it seems difficult to accept a source mechanism located in weak field regions, such as the neutral sheet, where this anisotropy would have to be continuously constrained within pitch angles less than about ½ degree to the magnetic field vector.

It also appears that the bursts exist on field lines which are both closed and open, or at least extend to large distances into the tail region. In an analysis based upon IMP 1, 2 and 3 magnetic field measurements and the continuity of magnetic lines of force ($\nabla \cdot \vec{B} = 0$), Fairfield

(1968) has mapped the positions on the equatorial plane of field lines emanating from the earth at various latitudes and local times. From this map one can determine the transition latitudes between closed and "open" field lines, especially in the noon hemisphere. In Table 2 we show the latitude of this transition for various local times and the high and low latitude boundaries of the burst region, obtained from Figure 8. In all cases the bursts exist well to each side of the transition latitudes.

As previously mentioned it is not possible to determine from the particle data alone whether the bursts are spatial or temporal in nature. Observations from some other experiment are required to distinguish between the two possibilities, but to date only the photometric data of short lived optical emissions observed from a jet aircraft by Eather (1969) may be relevant. The duration of these "spike precipitation events" was typically 75 to 100 seconds, which if they are interpreted to be spatially stable with the aircraft flying under the forms would correspond to widths of 20 to 25 km, or 3 to 4 seconds in the frame of reference of the satellite. Thus if there is a correspondence between these optical events and our burst type precipitation, this observation of Eather suggests a spacial rather than temporal nature of the bursts.

CONCLUDING REMARKS

This paper has presented a preliminary summary of observations of low energy electrons in the high latitude region by the Auroral Particles Experiment aboard the OGO-4 satellite. It was based on the first four months of data acquired from the experiment, which has collected data for 1½ years. Each of the items discussed will be studied more extensively,

especially in conjunction with other experiments aboard the Observatory, which provides the capability for the interdisciplinary study of geophysical phenomena. Ground level measurements made simultaneously with satellite passes could also be useful in the analysis, particularly to assist in the removal of the spatial/temporal ambiguity in the satellite data, but also to provide measurements of phenomena associated with particle influxes, and to expose the relationships between satellite and ground based synoptic studies.

ACKNOWLEDGEMENTS

I would like to thank Drs. D. S. Evans and D. J. Williams for beneficial discussions, and Mr. Fred Berko for very significant data analysis and programming assistance.

REFERENCES

Burch, J. L., Low-energy electron fluxes at latitudes above the auroral zone, J. Geophys. Res., 73, 3585, 1968.

Burch, J. L., Satellite measurements of low energy electrons precipitated at high latitudes, NATO Advanced Study Institute, Tretten, Norway, 1969.

Eather, R. H., Latitudinal distribution of auroral and airglow emissions: The "soft" auroral zone, J. Geophys. Res., 74, 153, 1969.

Fairfield, D. H., The average magnetic field configuration of the outer magnetosphere, J. Geophys. Res., 73, 7329, 1968.

Feldstein, Y. I., A. D. Schevnin, and G. V. Starkov, Auroral oval and magnetic field in the tail of the magnetosphere, The Birkeland Symposium on Aurora and Magnetic Storms, ed. A. Egeland and J. Holtet, Centre National de la Recherche Scientifique, 1967.

Hoffman, R. A., Low-energy electron precipitation at high latitudes, J. Geophys. Res., 74, 2425, 1969.

Hoffman, R. A., and D. S. Evans, OGO-4 auroral particles experiment and calibrations, Goddard Space Flight Center Preprint, X-611-67-632, 1967.

Hoffman, R. A., and D. S. Evans, Field aligned electron bursts at high latitudes observed by OGO-4, J. Geophys. Res., 73, 6201, 1968.

Maehlum, B., Universal-time control of the low energy electron fluxes in the polar regions, J. Geophys. Res., 73, 3459, 1968.

Maehlum, B., On the high latitude, universal-time controlled F layer, J. Atm. Terrest. Phys., 1969.

Sharp, R. D., and R. G. Johnson, Satellite measurements of auroral particle precipitation, Earth's Particles and Fields, ed. B. M. McCormac, 113, Reinhold Book Corp., Chicago, 1963.

FIGURE CAPTIONS

Figure 1. Schematic diagram of the experiment detector system indicating the look directions of the detectors with respect to the earth radius vector, the center energies measured by each detector, and the sampling scheme of the detector outputs, where the blackened area indicates the accumulation period.

Figure 2. Responses of the 0.7 kev and 7.3 kev detectors to precipitating electrons in the northern hemisphere during a dusk to dawn polar crossing. (K_p = 0+).

Figure 3. Responses of the 0.7 kev and 7.3 kev detectors to precipitating electrons in the northern hemisphere near midnight. (K_p = 1-).

Figure 4. An example of burst activity at invariant latitudes above 80° near local noon in magnetic local time. The telemetry rate was 4 bbps.

Figure 5. Highest resolution data available from the spacecraft. These bursts occurred at about 03 hours magnetic local time at a latitude of 69°.

Figure 6. Counting rates of the four detectors with common center energy of 2.3 kev and angles with respect to the radius vector from the earth of 0°, 30°, 60° and 90°. These data were taken at about 21 hours magnetic local time at an invariant latitude of 70° at a telemetry rate of 4 bbps.

Figure 7. Pitch angle distributions of the first two bursts in Figure 6.

Figure 8. A map of the probability of occurrence of bursts (F) for magnetic activity having $K_p \leq 2$. See text for the criteria used in defining bursts.

Figure 9. Same as Figure 8 for $K_p > 2$.

Figure 10. A scatter plot of the total counts within a burst as measured by the 0° detector versus the total counts measured by the 60° detector.

TABLE 1

Center Energy of Detector (kev)	Conversion Factor* (to $\frac{\text{electrons}}{\text{cm}^2\text{-sec-ster-kev}}$)
0.7	6.70×10^5
2.3	2.03×10^5
7.3	8.13×10^4
24.8	3.60×10^4

* to convert from counts/readout for the 4 kilobit/sec tape storage mode of the spacecraft. For 16 kilobits/sec. telemetry rate these factors must be multiplied by 4.

TABLE 2

Magnetic Local Time	Transition Latitude	Low Latitude Boundary	High Latitude Boundary
12	77	75	85
08	77	72½	≥ 85
16	77	72½	≥ 82½
04	73	70	≥ 77½
20	73	67½	≥ 80
24	69	≤ 67½	75

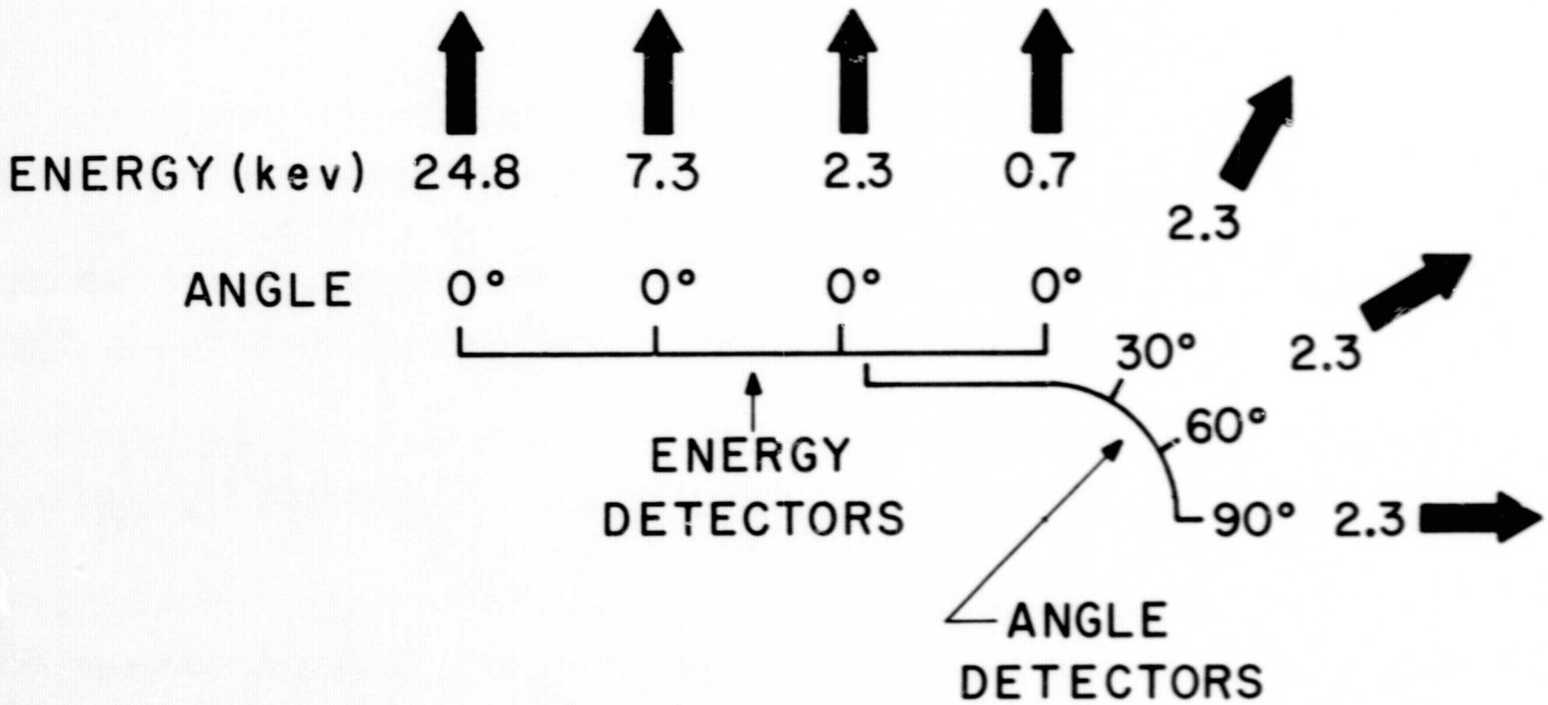
ENERGY (kev) 24.8 7.3 2.3 0.7
2.3
ANGLE 0° 0° 0° 0°
30° 2.3
60°
90° 2.3
ENERGY DETECTORS
ANGLE DETECTORS

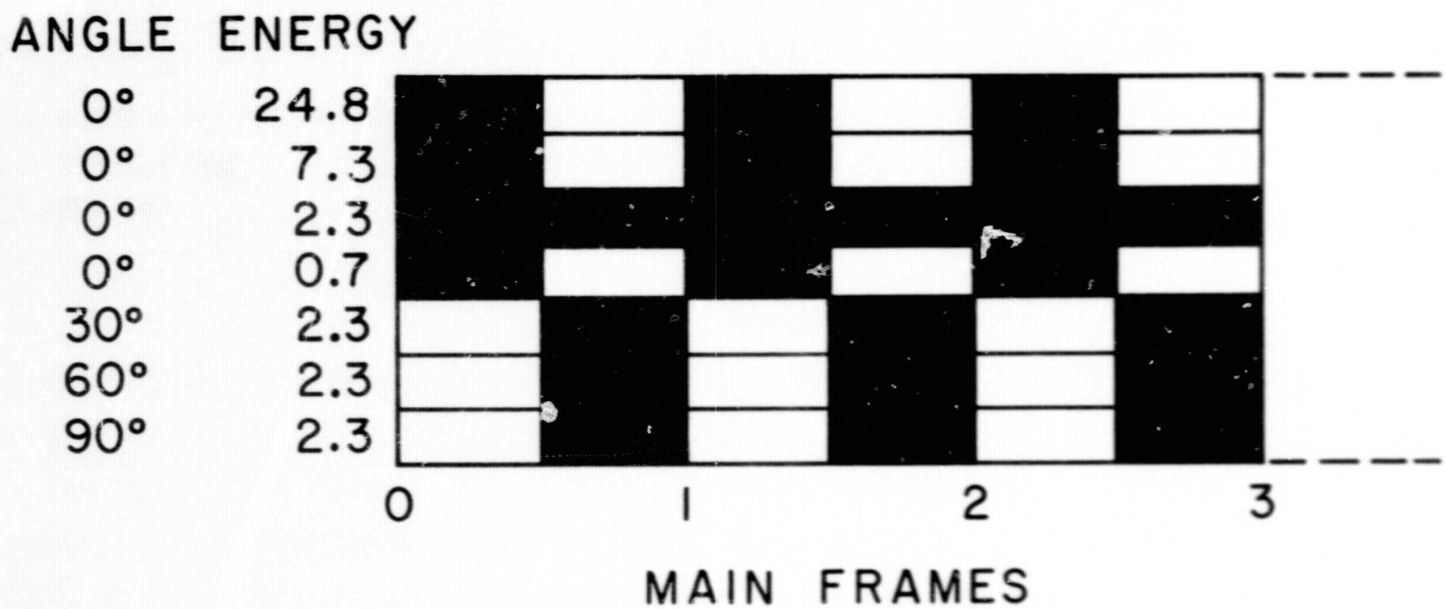
ANGLE ENERGY
0° 24.8
0° 7.3
0° 2.3
0° 0.7
30° 2.3
60° 2.3
90° 2.3
0 1 2 3
MAIN FRAMES

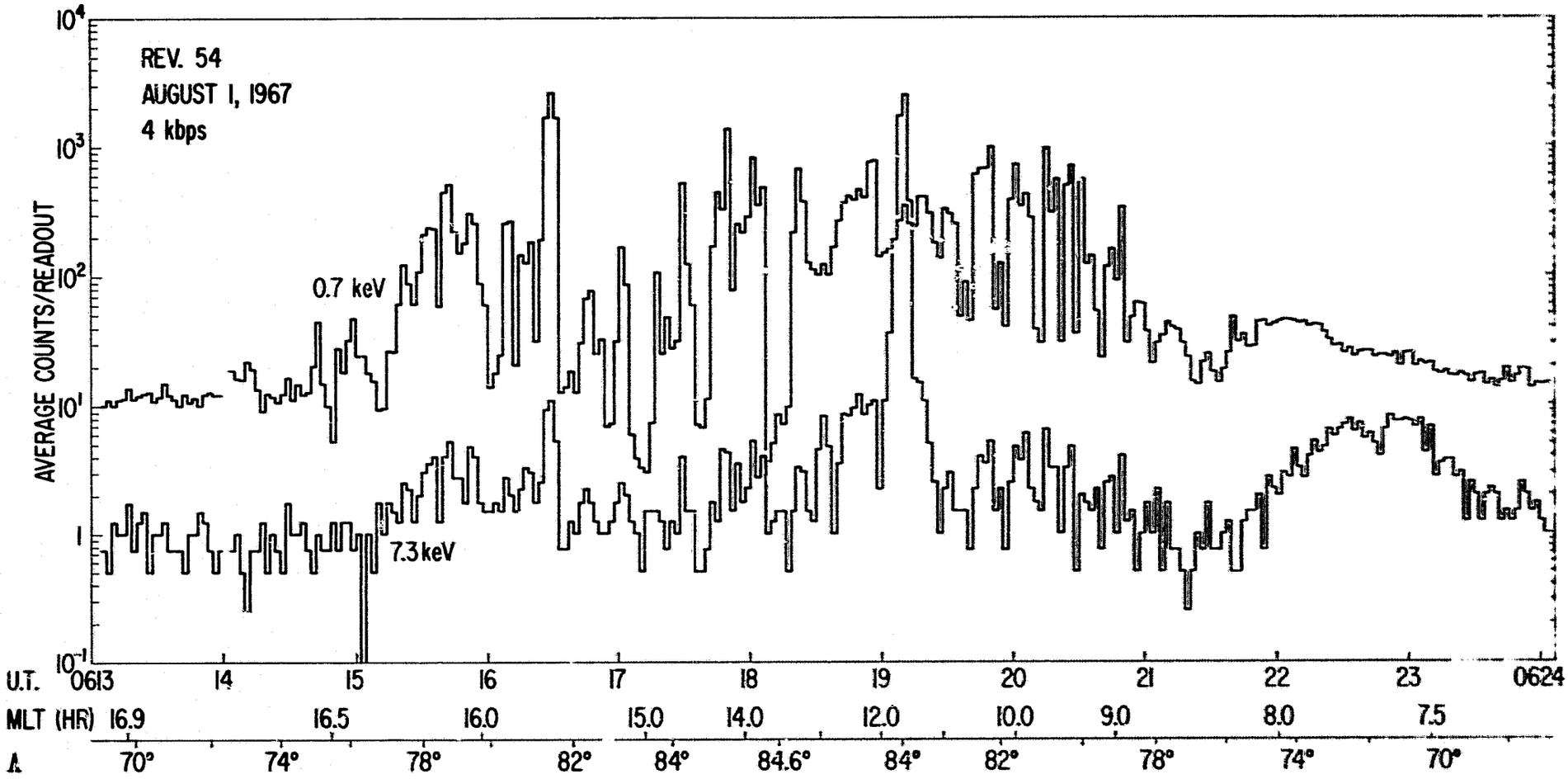
REV. 54
AUGUST 1, 1967
4 kbps
0.7 keV
7.3 keV
AVERAGE COUNTS/READOUT
10^4
10^3
10^2
10^1
1
10^{-1}
U.T. 0613 14 15 16 17 18 19 20 21 22 23 0624
MLT (HR) 16.9 16.5 16.0 15.0 14.0 12.0 10.0 9.0 8.0 7.5
Λ 70° 74° 78° 82° 84° 84.6° 84° 82° 78° 74° 70°

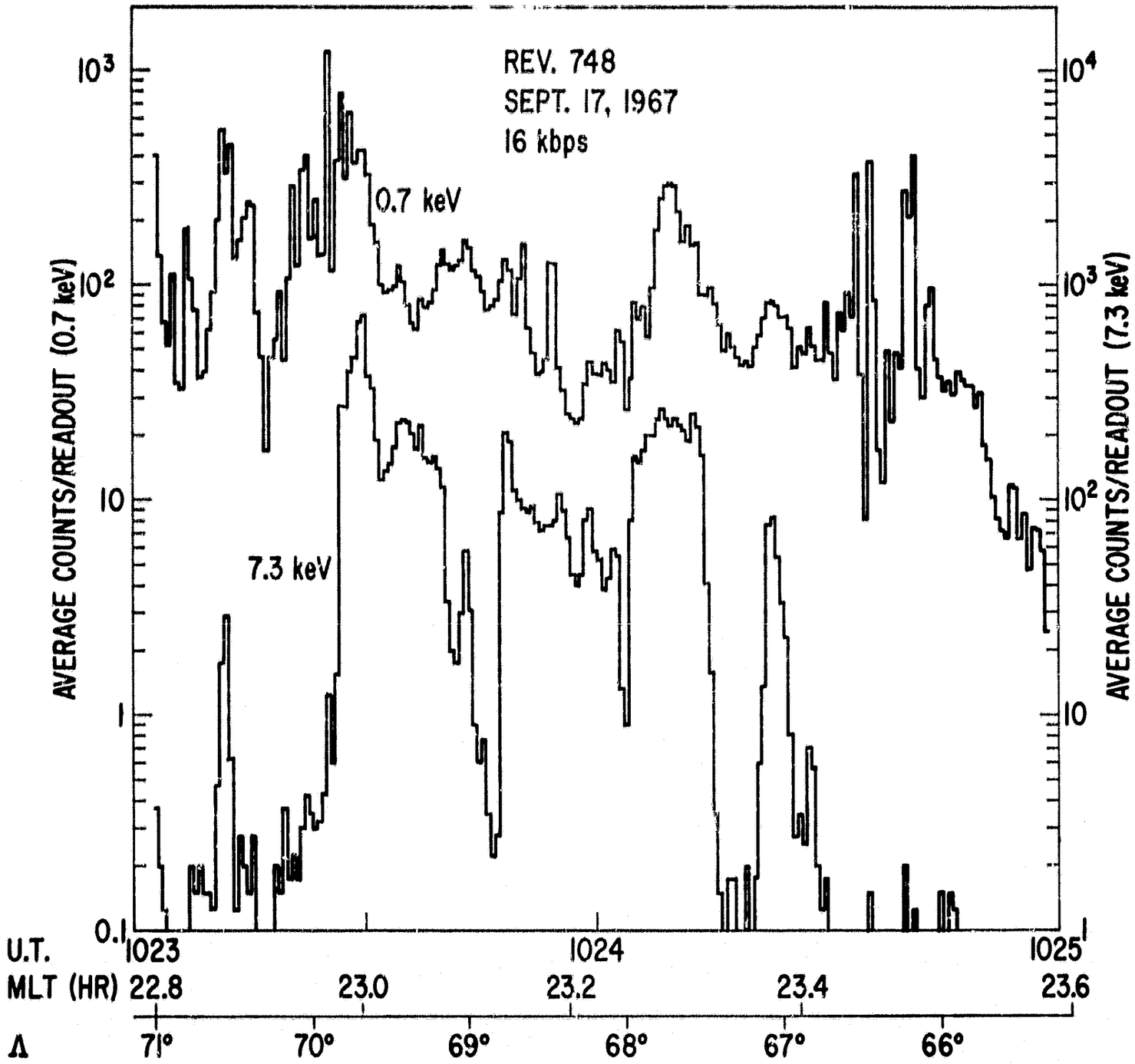
REV. 748
SEPT. 17, 1967
16 kbps
0.7 keV
7.3 keV
AVERAGE COUNTS/READOUT (0.7 keV)
AVERAGE COUNTS/READOUT (7.3 keV)
10^3
10^2
10
1
0.1
10^4
10^3
10^2
10
1
U.T.
1023
1024
1025
MLT (HR)
22.8
23.0
23.2
23.4
23.6
Λ
71°
70°
69°
68°
67°
66°

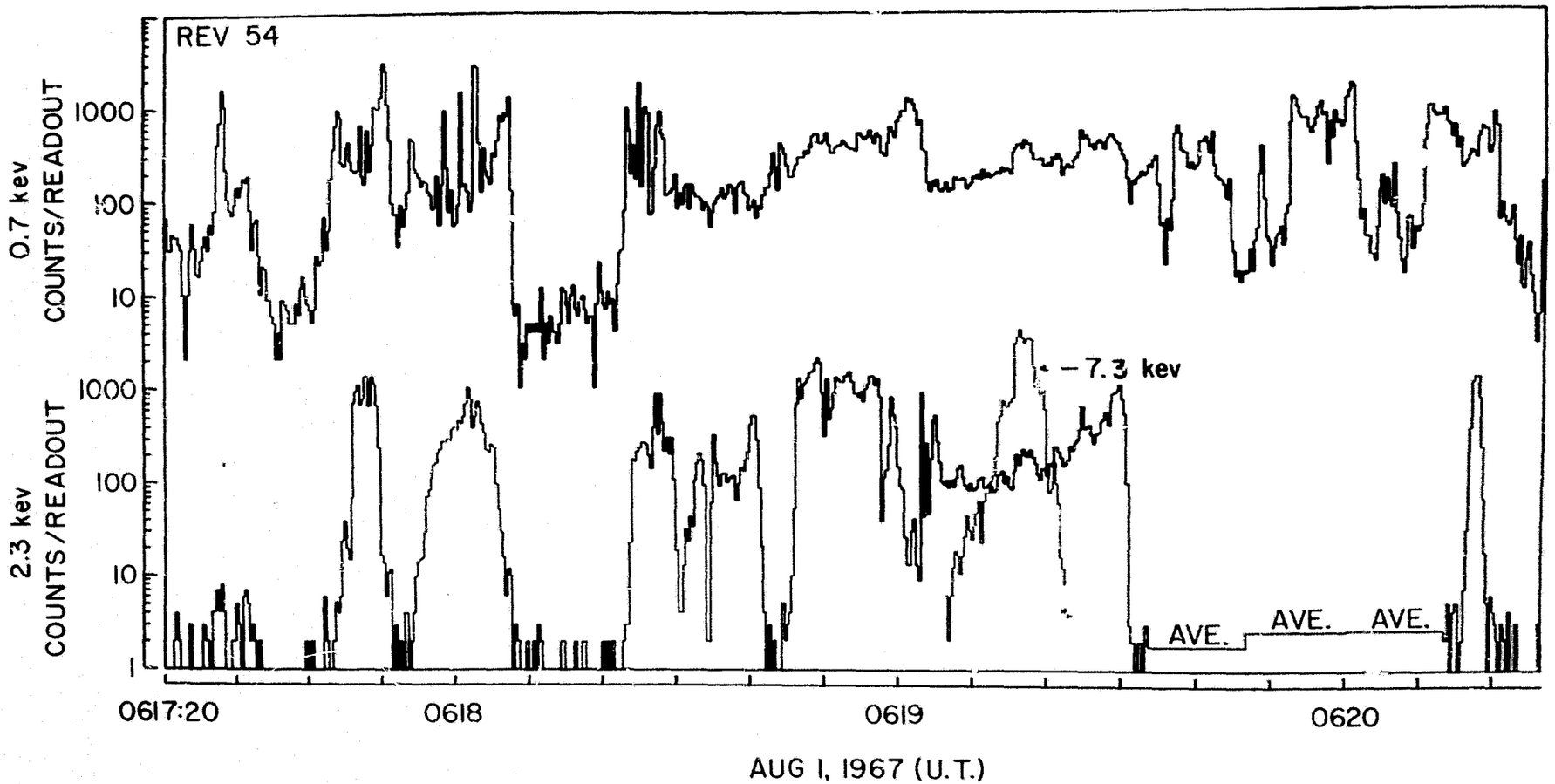
REV 54
0.7 kev
COUNTS/READOUT
1000
100
10
2.3 kev
COUNTS/READOUT
1000
100
10
1
7.3 kev
AVE.
AVE.
AVE.
0617:20
0618
0619
0620
AUG 1, 1967 (U.T.)

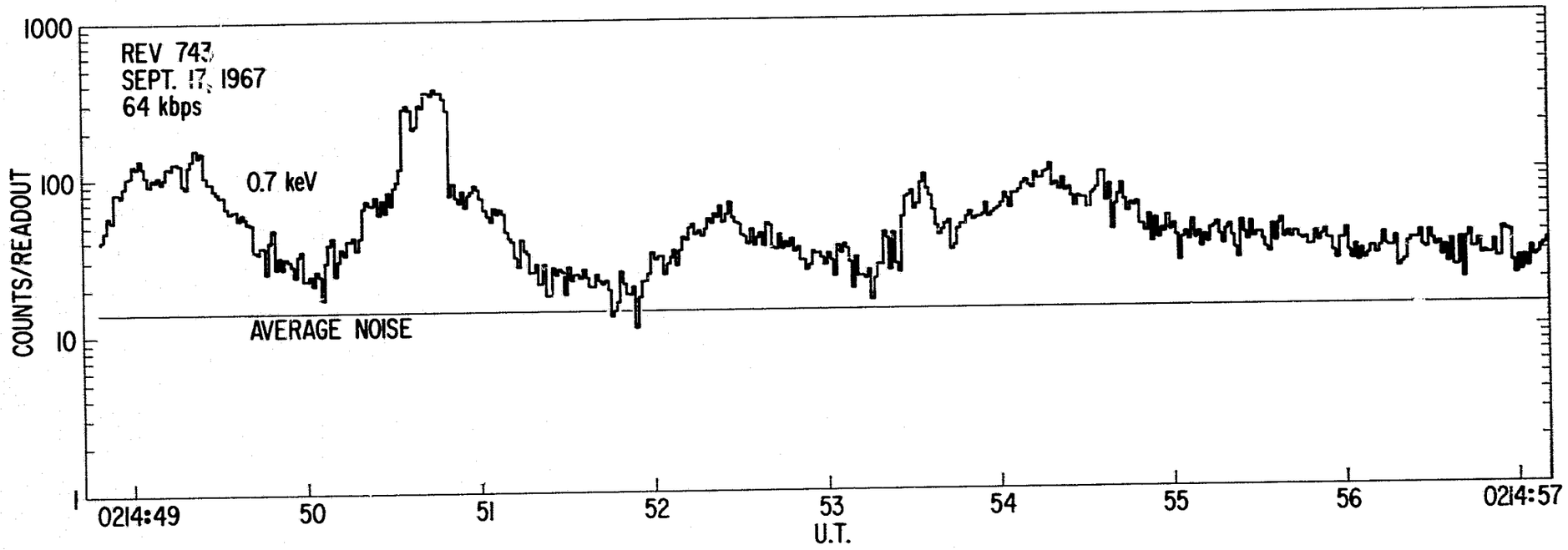
REV 743
SEPT. 17, 1967
64 kbps
0.7 keV
AVERAGE NOISE
COUNTS/READOUT
1000
100
10
1
0214:49
50
51
52
53
54
55
56
0214:57
U.T.

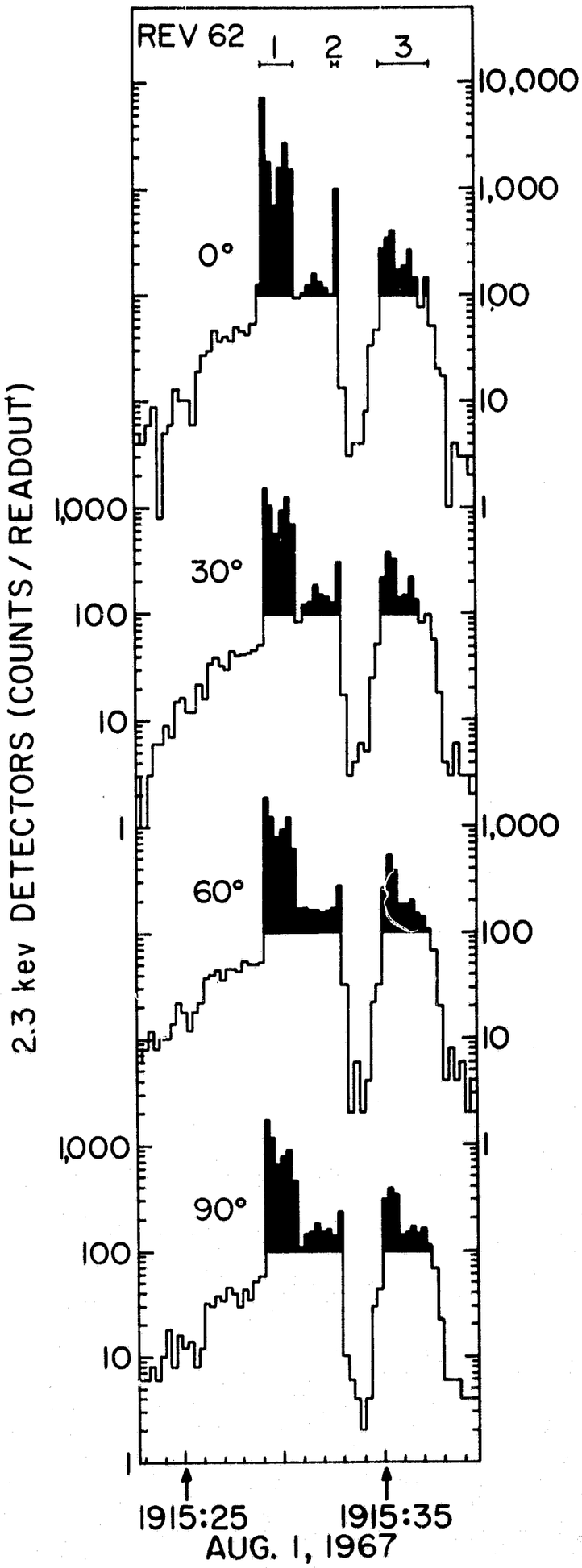
REV 62
1
2
3
0°
30°
60°
90°
10,000
1,000
100
10
1
1,000
100
10
1
1,000
100
10
1
1,000
100
10
1
2.3 kev DETECTORS (COUNTS / READOUT)
1915:25
1915:35
AUG. 1, 1967

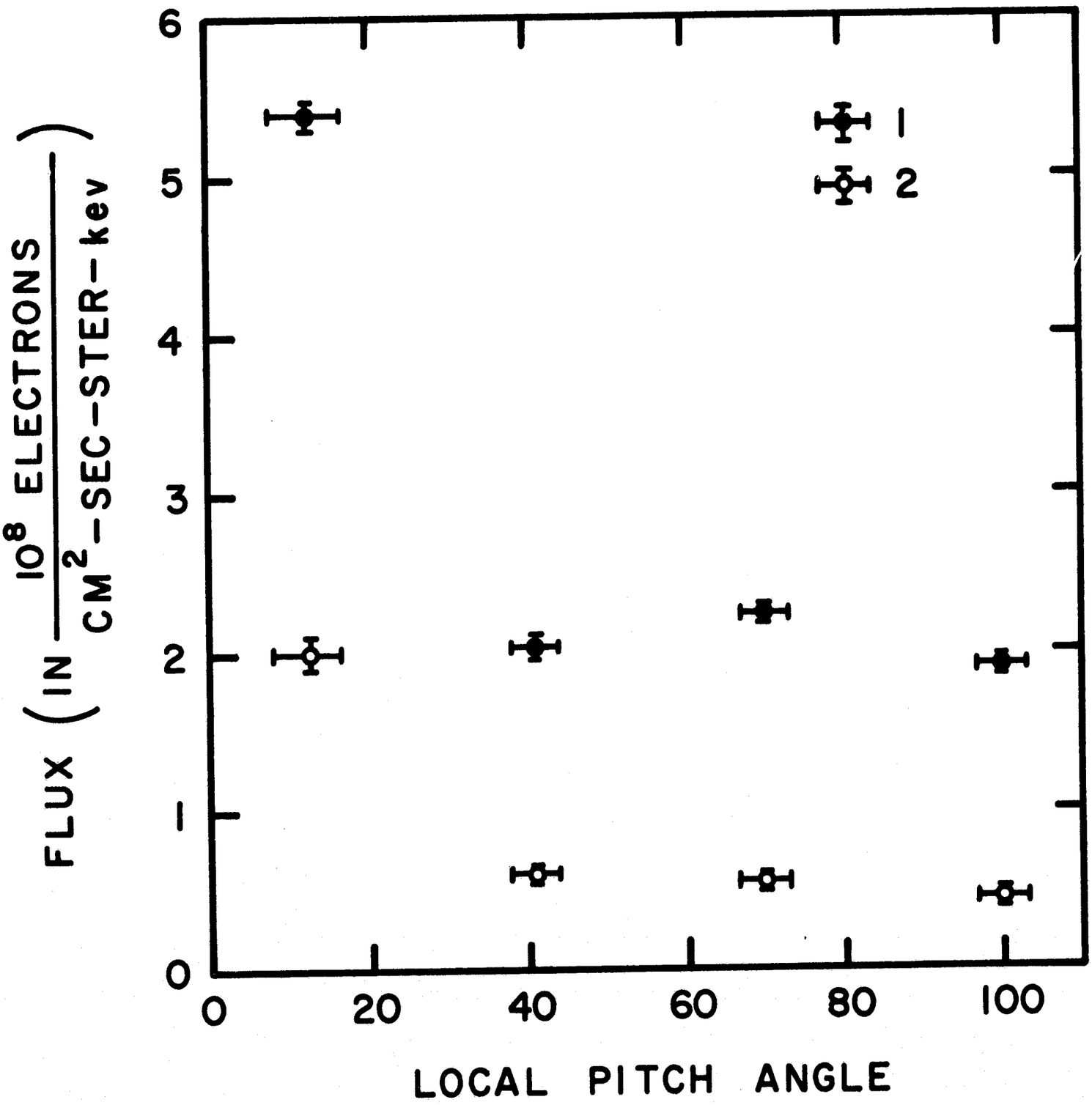
FLUX (IN $\frac{10^8 \text{ ELECTRONS}}{\text{CM}^2\text{-SEC-STER-kev}}$)
6
5
4
3
2
1
0
0
20
40
60
80
100
LOCAL PITCH ANGLE
1
2

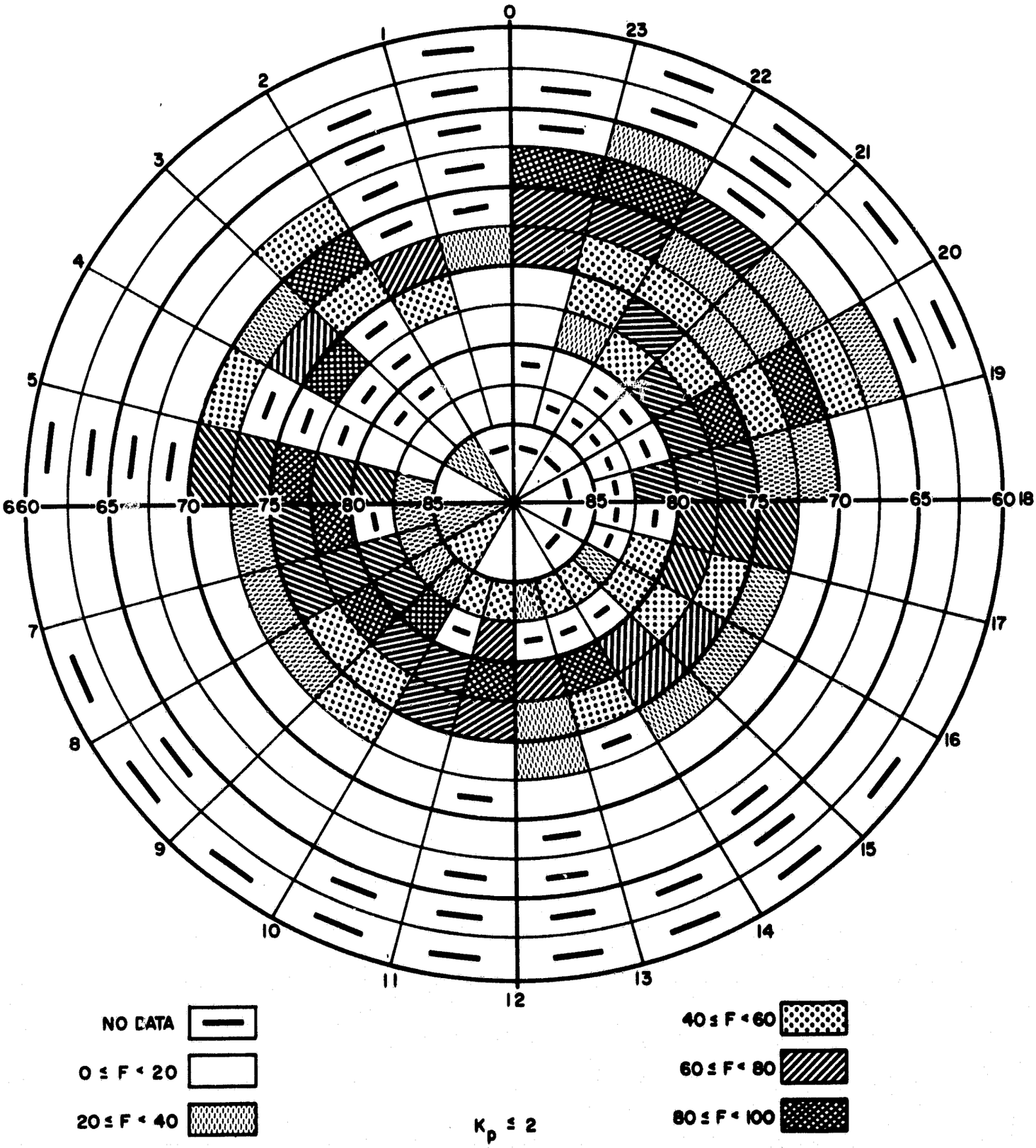
0
1
2
3
4
5
6
7
8
9
10
11
12
13
14
15
16
17
18
19
20
21
22
23
60
65
70
75
80
85
85
80
75
70
65
60
NO DATA
0 ≤ F < 20
20 ≤ F < 40
40 ≤ F < 60
60 ≤ F < 80
80 ≤ F < 100
$K_p \leq 2$

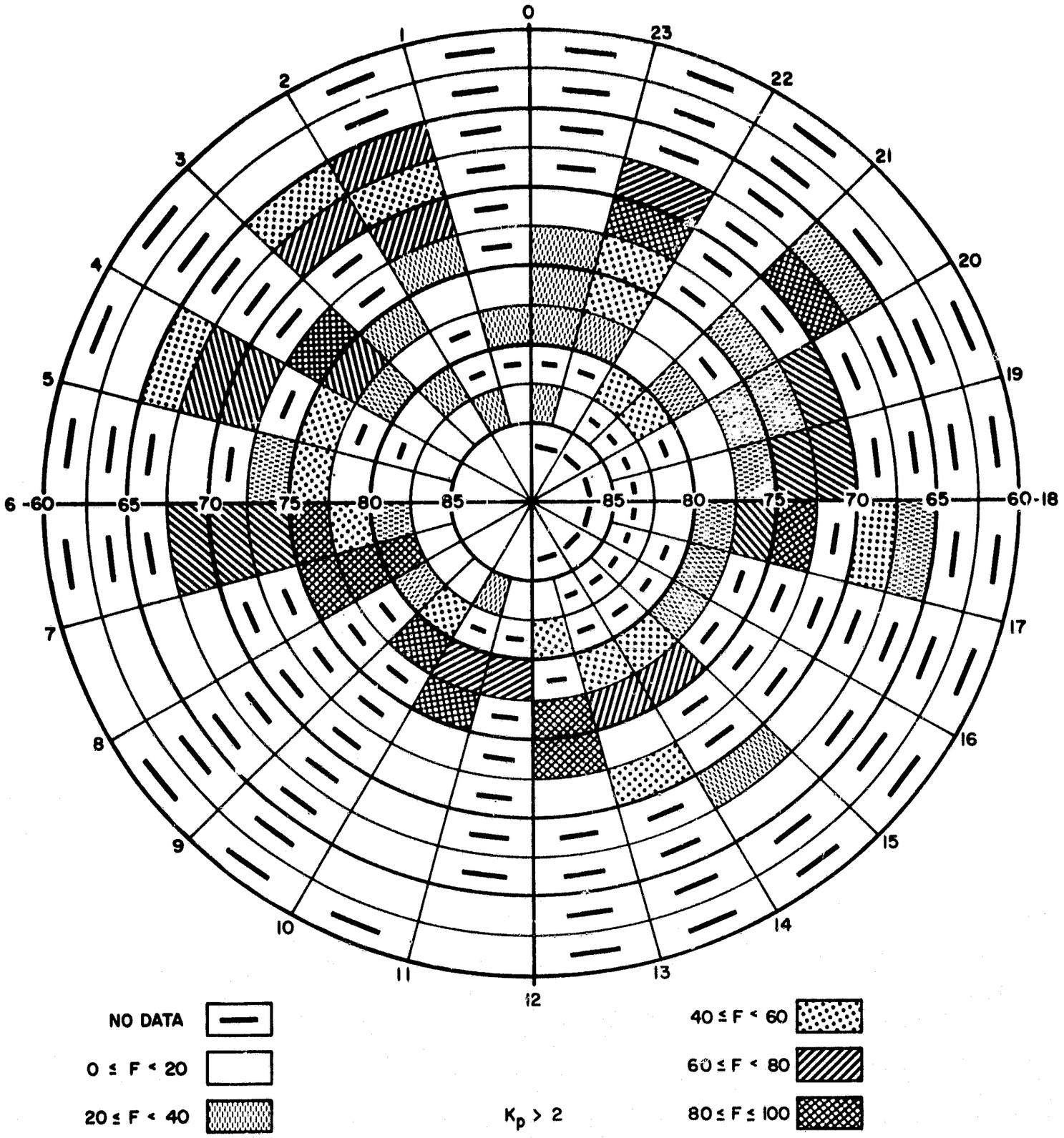
0
1
2
3
4
5
6
7
8
9
10
11
12
13
14
15
16
17
18
19
20
21
22
23
60
65
70
75
80
85
85
80
75
70
65
60
NO DATA
0 ≤ F < 20
20 ≤ F < 40
40 ≤ F < 60
60 ≤ F < 80
80 ≤ F ≤ 100
$K_p > 2$

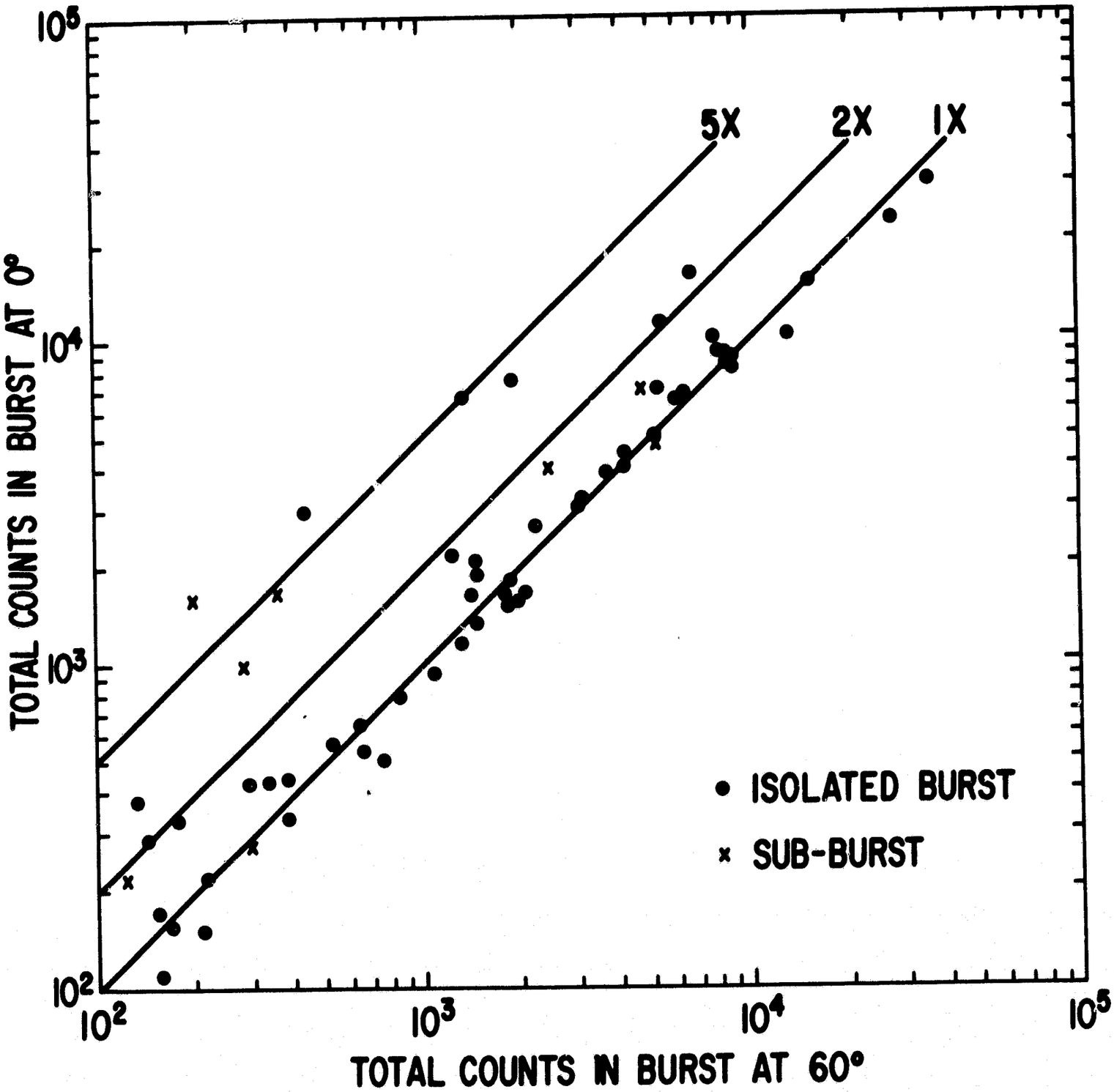
5X
2X
1X
ISOLATED BURST
SUB-BURST
TOTAL COUNTS IN BURST AT 0°
TOTAL COUNTS IN BURST AT 60°
10^2
10^3
10^4
10^5